ARCHIVE OF MECHANICAL ENGINEERING

DOI: 10.24425/ame.2022.140420 2022, Vol. 69, No. 3, pp. 519–539

Van-The THAN [1], Chi-Chang WANG [2], Thi-Thao NGO [1], Guan-Liang GUO [2]

Applying rapid heating for controlling thermal displacement of CNC lathe

Received 12 November 2021, **Revised** 8 February 2022, **Accepted** 16 February 2022, **Published online** 6 May 2022

Keywords: rapid heating, CNC lathe, thermal displacement, ball screw, temperature control

Thermal error always exists in a machine tool and accounts for a large part of the total error in the machine. Thermal displacement in X-axis on a CNC lathe controlled based on a rapid heating system is presented in this paper. Positive Temperature Coefficient (PTC) heating plates are installed on the X-axis of the machine. A control temperature system is constructed for rapid heating which further helps the thermal displacement to quickly reach stability. The system then continuously maintains stable compensation of the thermal error. The presented rapid heating technique is simpler than the compensation of machine thermal errors by interference in the numerical control system. Results show that the steady state of the thermal displacement in the X-axis can be acquired in a shorter time. In addition, thermal errors in constant and varying working conditions could be significantly reduced above 80% and 60%, respectively, compared to those without using the rapid heating. Therefore, the proposed method has a high potential for application on the CNC lathe machine for improving its precision.

Nomenclature

c	specific heat, J/(kg K)
C	temperature control parameter
h	convection coefficient, W/(m^2 °C)
k	thermal conductivity, W/(m K)
Nu	Nusselt number

✉ Van-The Than, e-mail: thanthe.ck@gmail.com

[1]Faculty of Mechanical Engineering, Hung Yen University of Technology and Education, Khoai Chau District, Hung Yen Province, Vietnam. ORCID V.T.T.: 0000-0002-2144-6963

[2]Department of Mechanical and Computer-Added Engineering, Feng Chia University, Taichung, Taiwan, R.O.C.

Pr	Prandtl number
$\dot{q}$	heat flux per volume, W/m^3
r_t	steady-state time improvement rate, %
r_δ	maximum displacement improvement rate, %
T	temperature, °C
ΔT	temperature increment, °C
t	time, min

Greek symbols

δ	thermal displacement, μm
ε	emissivity
ρ	density, kg/m^3
σ	standard deviation

Subscripts

C	control temperature
f	fast heating
fast	total time of fast heating
max	maximum value
min	minimum value
o	no fast heating
∞	ambient temperature

1. Introduction

Machining efficiency and accuracy of machine tools are key factors of machine tool price. However, the machine tool assembled by a lot of parts is heated up and expands (i.e., thermal displacement) under high-speed cutting condition; expanding parts further affect manufacturing accuracy of the machine tools. In 1990, Bryan [1] indicated that the thermal error accounted for 40-70% of the total machine tool error. Some researchers have tried to find the way of reducing the thermal displacement. In 2012, Mayr et al. [2] measured the temperature and displacement of a machine tool and they built a thermal model based on experimental data to calculate the thermal error. Their results showed that the thermal errors determined through thermal expansion of machine components and the workpiece were closely related to machine tool thermal behavior. As it is known, the thermal expansion coefficient of carbon steel (screw of S45C) is 12E-6(1/°C). Therefore, thermal expansion of a meter length due to temperature increase of 1°C equals about 12 μm. Hence, the thermal displacement of a machine tool significantly influences machine precision.

In a CNC lathe machine, the thermal expansion of the screw will cause inaccuracy of the turret positioning during operation. The thermal behavior during raising temperature also affects the turret position and the overall machine tool accuracy. Wang et al. [3] presented a thermodynamic model based on thermal characteristics of ball screws. They proposed equations to estimate friction torque and heat generation and then built a thermal model based on the lumped heat-capacity method. Jin et al. [4] analyzed a ball bearing and reported that sharp temperature rise of the bearing was mostly induced by friction which further generates heat. The friction magnitude depends on working conditions including the internal load, the contact angle, the rotational speed and the external load. In order to enhance simulation accuracy of thermo-property analysis model, Liu et al. [5] proposed a method with optimized thermal boundary conditions. They then tested the ball screw under different feed rates to validate the effectiveness of their method. Wu and Kung [6] used thermocouple and laser interferometer to measure temperature and thermal error, respectively. The finite element method was also used to analyze temperature and thermal deformation of the ball screw feeding system. Simulated and experimental results were compared for different feed rates. Shi et al. [7] analyzed thermal error between the screw and the driving system. Results indicated that the thermal error varied according to the working position with changing the ball screw length and the working time. Yun [8] divided the driving system into the ball screw and the guide rail and developed thermal behavior models for them. Position errors of the feed drive system caused by thermal expansion were estimated. Moreover, a lumped heat-capacity method and a genius education algorithm were adopted in this study to analyze the linear positioning error of the ball screw. From the above literature review, it is clear that different feed rates result in heat generation from the ball screw as well as the guide rail, which may significantly affect the accuracy of the machine tool. Therefore, controlling the thermal expansion of the screw can help improving precision of the machine tool.

Currently, the thermal accuracy of machine tools is mostly improved by using thermal suppression or developing thermal compensation models. Shi [9] and Xu [10] used oil and air cooling for a ball screw and employed finite element analysis to consider the effect of flow inside a cored screw on its temperature. A relationship between the heat convection coefficient and cooling system parameters was determined. Results indicated that the flow velocity of the internal fluid had a significant effect on thermal suppression. In addition, the running ball screw could reach thermal equilibrium earlier and the positioning accuracy could be improved. However, thermal suppression sometimes creates high cost which can lead to the increase in overall machine tool price. Thermal compensation method is widely investigated by researchers. Huang [11] adopted multiple linear regression to build the model of ball screw, and selected heat source generated from the front bearing, the nut and the back bearing as the variables of his model. Li et al. [12] proposed a time-varying reliability model, and proved the validity of the model by using the ball screw feeding system. Ma et al. [13] presented a thermal error modeling and compensation method for ball screws. They proposed a closed-loop iterative thermal behavior modeling method. The multiple linear regression analysis is applied to compensate for thermal error under different working conditions. The results indicated that thermal errors were significantly reduced. Zapłata et al. [14] employed a partial differential equation to model temperature distribution for compensating the thermal error of ball screw. They showed that the feed rate was related to the variance in model parameters; nevertheless, the accuracy was lower than the thermal displacement compensation based on temperature measurement. Feng et al. [15] mentioned a method for calculating the temperature during preheating. In order to solve the non-uniform heat distribution of a screw, they divided the screws into several uniformly-distributed heat regions for modeling. The results revealed that the overlapped thermal model for compensation could enhance the machine tool accuracy effectively. Zhou et al. [16] used a real-time data including current, speed and feeding of the CNC system for building a thermal compensation model. The parameters of their proposed model were determined through multiple linear regression method. Then, the model was validated by the ball screw on a small machine tool.

From above analysis, it is indicated that the thermal error is mostly removed by thermal compensation and thermal suppression. However, both of them require a lot of experimental time and a high-cost equipment. Most scholars have analyzed the thermal behavior of the ball screw; and they indicated that thermal displacement of the screw significantly influences the accuracy of turret position. In this paper, a fast heating is proposed to control the temperature on the ball screw, which further results in reaching a stability of thermal displacement on the X-axis in a short time. Therefore, moving accuracy of the turret could be enhanced and finally the machine tool precision could be improved.

2. Experimental construction and mathematical method

A CNC horizontal lathe with 4200 rpm of maximum spindle speed is used to perform experiments (Fig. 1). The maximum working regions of the X- and Z-axis of the machine are 150 mm and 250 mm, respectively. Fig. 2 shows the diagram of a rapid heating system, which is divided into two groups, including fast-heating control module, and displacement and temperature measurement. They will be presented more detail in this section.

2.1. Temperature and displacement measurement

In order to command heating power control, temperature information needs to be collected and fed back to the central processor. In addition, thermal displacements in the workpiece are also recorded; while, the variation of thermal displacement from the start to the steady state of the machine tool is determined by fluctuation of the distance between the turret and the workpiece. As shown in Fig. 1, eight temperature sensors are attached to the lathe machine and descriptions of temperatures in these points are listed in Table 1. There are two thermocouples (T_1 and T_2) located on the heating plates for giving temperature information and a feedback to the processor. Other six thermocouples are used to observe variation of the temperature on the whole machine as well as the ambient tem-

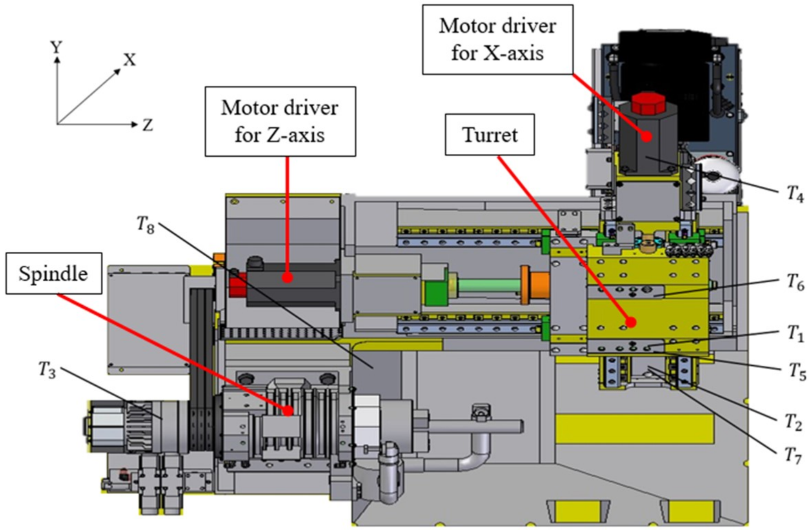

Fig. 1. Experimental machine tool and locations of thermocouples

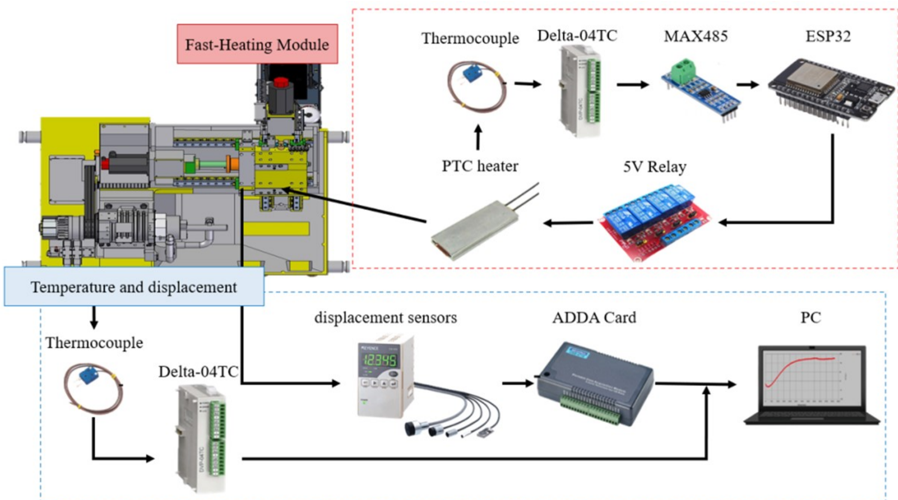

Fig. 2. The whole experimental structure

perature. This study adopts the Delta-04TC temperature module and the T-type thermocouple with measurement error less than 0.1°C to obtain the temperatures at demanded locations. To acquire thermal displacement data, a non-contact eddy-current displacement meter is employed in this work. The KEYENCE EX-305V sensor has a resolution that can reach 0.4 µm. Therefore, it is capable of measuring the thermal displacement in the machine tool which is mostly between 1 and 100 µm. The eddy-current displacement meter is fixed on the tool holder, and the

Table 1. Locations of measurement temperatures

Fast heating control temperature point		Temperature point for observation	
Name	Location	Name	Location
T_1	X-axis back bearing heating plate	T_3	spindle motor
T_2	X-axis saddle heating plate	T_4	X-axis motor
		T_5	X-axis back bearing
		T_6	X-axis screw
		T_7	X-axis saddle
		T_8	temperature inside machine

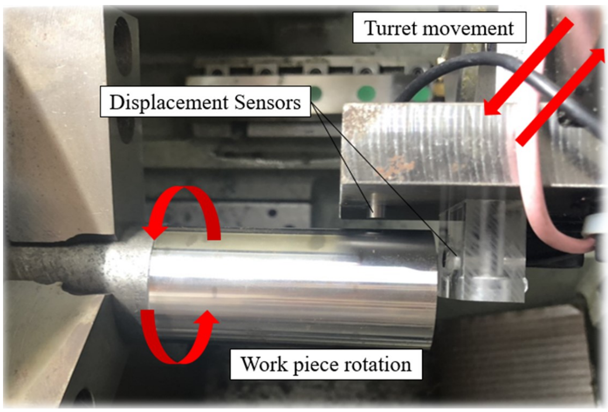

Fig. 3. Setting up displacement sensors

workpiece is rotated based on the spindle, as seen in Fig. 3. The relative displacement between the tool holder and the workpiece is captured during the spindle rotation.

2.2. Rapid heating control module and algorithm

In the rapid heating control module, the heating plate PTC is attached in machine bed and in the bearing support to generate heat for increasing the temperature of the end of the ball-screw system. A thermocouple is used to record temperature at the bearing support. The temperature, send back to a Delta-04TC temperature acquisition unit, is continuously transferred to the MAX-485 communication module and finally connected to the Microprocessor Control Unit (ESP32) to give logical decision for the magnitude of heating power. After processing, the Microprocessor Control Unit sends commands to the Relay Module for opening the circuit to the PTC heating plate. The whole fast-heating module is designed as a closed system that is automatically implemented to help the target temperature reaching the setting temperature (Fig. 4). Fig. 5 displays a flowchart of the rapid heating temperature control algorithm. Its operation consists of two stages, including the short-term rapid heating process and the long-term temperature control process.

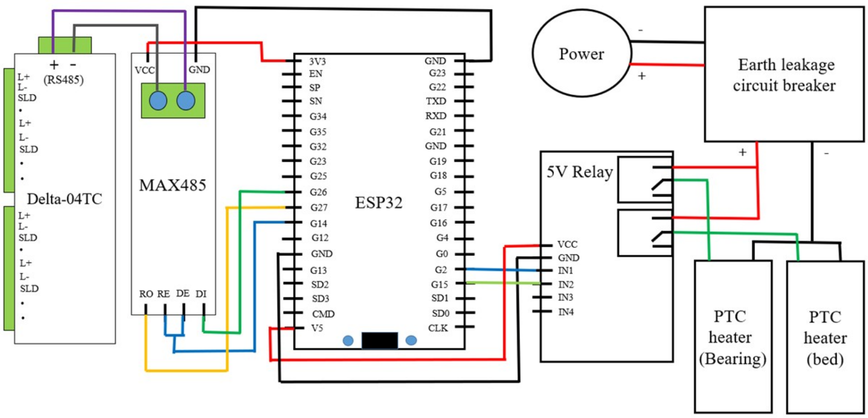

(a) Circuit diagram

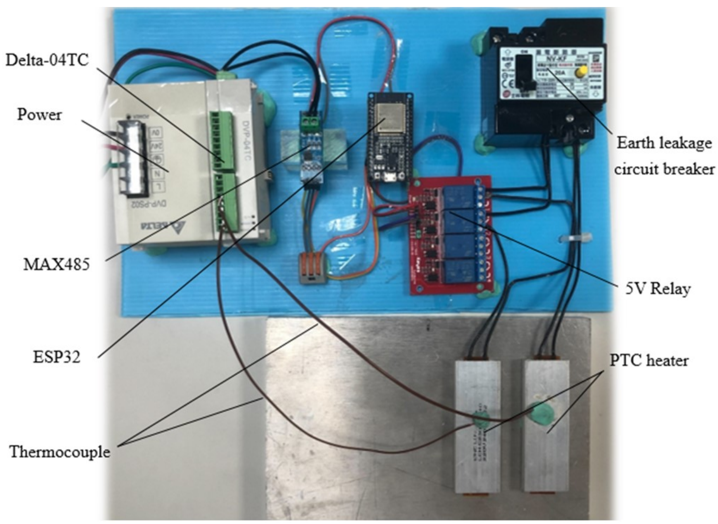

(b) Equipment system

Fig. 4. Schematic diagram of rapid heating temperature control module

For stage 1: short-term rapid heating process

Before working, machine tools often need time to start up the systems such as oil pumps, compressed air etc., and especially to warm up to minimize the thermal error. With the rapid heating method, the temperature of a machine tool can reach a steady state in a short time that may further help the machine to acquire a stable thermal displacement. In the machine in Fig. 1, the heating time t_{fast} can be set and the system controls the power supply to the PTC heating plate for rapidly heating the area around it. The heat is then transfer to other components in the machine tool, such as bed, bearing support, ball screw etc. In this way, the demanded temperature is acquired in a short time.

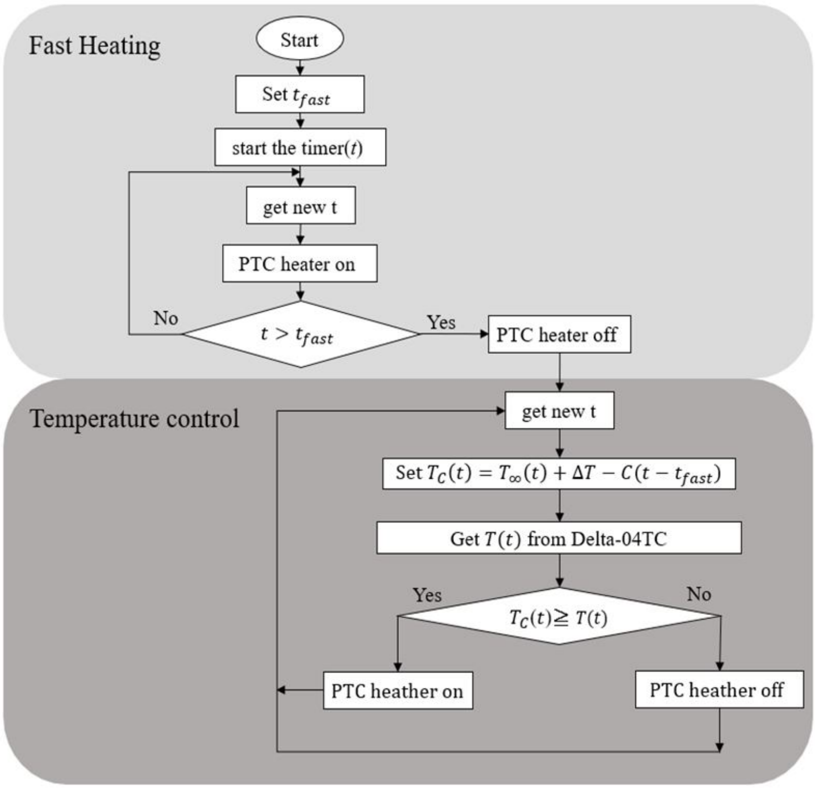

Fig. 5. Logic diagram of rapid heating and temperature control

For stage 2: Long-term temperature control process

After the rapid heating stage, the heat accumulated in the heating area is gradually transferred to peripheral components and to the environment, leading to temperature fall. Besides, there is an inevitable heat generation by different motors and bearings during the machine tool operation, which heats them up gradually. In this study, the cold and the hot sources which effect on steady state of the thermal displacement of the machine tool are investigated. However, approaching this steady state sometimes requires several hours. Therefore, the experiments presented in this paper aim at constructing temperature control of the heating plate after the rapid heating in stage 1. If the target value of the controlled temperature is $T_C(t)$, the relation could be expressed as follows:

$$T_C(t) = T_\infty(t) + \Delta T - C(t - t_{\text{fast}}), \tag{1}$$

where t, $T_\infty(t)$ and t_{fast} are the time elapsing from the start of experiment, the ambient temperature and the total rapid heating time of the heating plate in stage 1, respectively; ΔT and C are respectively the temperature increment and the temperature control coefficient. Using this algorithm, one can avoid the temperature after rapid heating, restore it to the original state quickly and gradually change towards the steady state. When the temperature of the heating plates is lower than $T_C(t)$, the heating process is turned on as long as the temperature reaches the required $T_C(t)$ (refer to Fig. 5).

During heating, temperature of the bearing may rapidly increase, which may cause an overheat phenomenon and further reduce life of the bearing. To consider this problem, a thermal model consisting of a bed, a bearing, a bearing support and a ball-screw is constructed to simulate the temperature change in the structure. Fig. 6 presents a 3D-thermal model that is then imported in the Comsol Multiphysics software for analyzing temperature not only inside the bearing but also temperature distribution over the whole structure. Four PTC heater plates are located in the bearing support as well as in the bed, and they are considered as the heat sources in the present simulation.

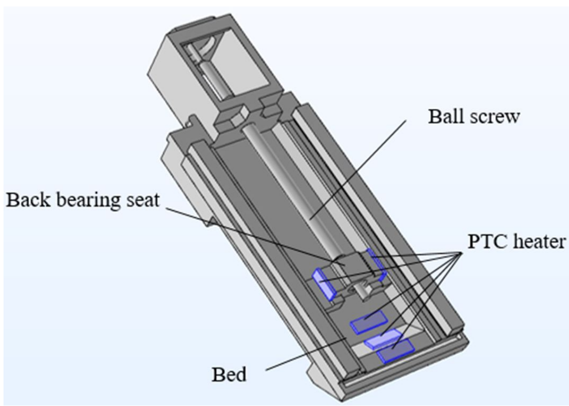

Fig. 6. Three-dimensional model of heating structure

The energy conservation equation of heat transfer for the structure can be expressed as

$$\rho c \frac{\partial T(t)}{\partial t} = k \left(\frac{\partial^2 T(t)}{\partial x^2} + \frac{\partial^2 T(t)}{\partial y^2} + \frac{\partial^2 T(t)}{\partial z^2} \right) + \sum_{i=1}^{5} \dot{q}_i(x, y, z, t), \tag{2}$$

where $T(t)$ and t represent the temperature and time respectively; ρ, c and k are, respectively, the density (7850 kg/m^3), specific heat (475 J/(kg K)) and thermal conductivity (44.5 W/(m K)) of AISI 4340 steel. $\dot{q}_i(x, y, z, t)$ is the heat generation of no. i heating plate distributed as in Fig. 6. The initial and boundary conditions are given by following equations:

$$T = T_\infty \quad \text{at} \quad t = 0, \tag{3}$$

$$k \frac{\partial T}{\partial n} = h(T_w - T_\infty) + \varepsilon\sigma(T_w^4 - T_\infty^4) \quad \text{on bed surface}, \tag{4}$$

where n, ∞ and w are the normal vectors of machine tool surface, and ambient and surface temperature, respectively; ε and σ stand for the object surface emissivity (Steel AISI 4340 set as 0.2) and the Boltzmann's constant (5.67E-8 W/(m^2 K^4)). h is the natural heat convection coefficient which can be calculated through the average Nusselt number ($\overline{\mathrm{Nu}}$), geometry parameter (D) and thermal conductivity of air (k_{air}) as follows:

$$h = \frac{\overline{\mathrm{Nu}} k_{\mathrm{air}}}{D} \tag{5}$$

for the rotational part, the average Nusselt number is estimated by [17]

$$\overline{\mathrm{Nu}} = 0.6366(\mathrm{Re}\,\mathrm{Pr})^{0.5}, \tag{6}$$

for natural convection, $\overline{\mathrm{Nu}}$ is determined as [18]

$$\overline{\mathrm{Nu}} = \begin{cases} 0.54\mathrm{Re}^{1/4} & 10^4 \leqslant \mathrm{Ra}_L \leqslant 10^7 & \text{on upper surface}, \\ 0.15\mathrm{Re}^{1/3} & 10^7 \leqslant \mathrm{Ra}_L \leqslant 10^{11} & \text{on upper surface}, \\ 0.27\mathrm{Re}^{1/4} & 10^5 \leqslant \mathrm{Ra}_L \leqslant 10^{10} & \text{on lower surface}, \\ 0.68 + \dfrac{0.67\mathrm{Ra}_L^{1/4}}{[1 + (0.492/\mathrm{Pr})^{9/16}]^{4/9}} & \mathrm{Ra}_L \leqslant 10^9 & \text{on vertical surface}. \end{cases} \tag{7}$$

All the above coefficients and heat sources are given as input parameters on thermal model in the Comsol software. Assuming that the heating time is equal to 10 minutes, the simulated temperature distribution on the bed, the screw, the bearing and on the other parts is obtained and displayed in Fig. 7. Variations of temperature with respect to time at three points, including inside the back bearing, on the back bearing and on the bed are derived and plotted in Fig. 8. The results show that maximum temperature on the back bearing (on the bearing's housing) is the highest one (about 53°C); about 42°C is the temperature of the bed, while

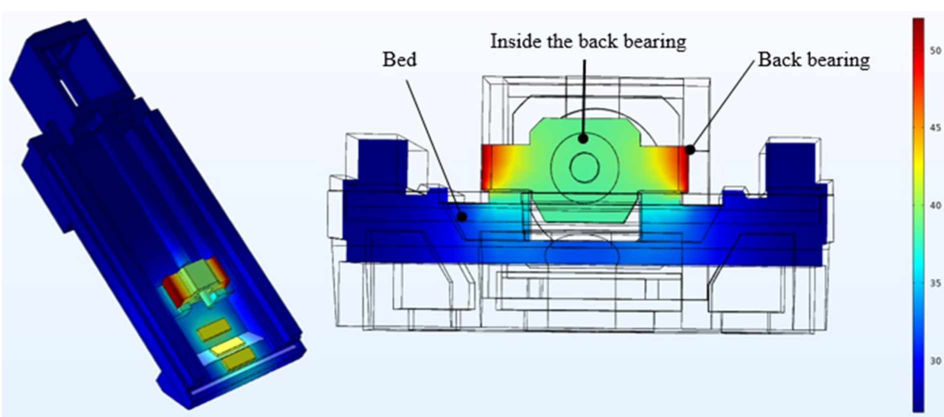

Fig. 7. Predicted temperature distribution on the structure

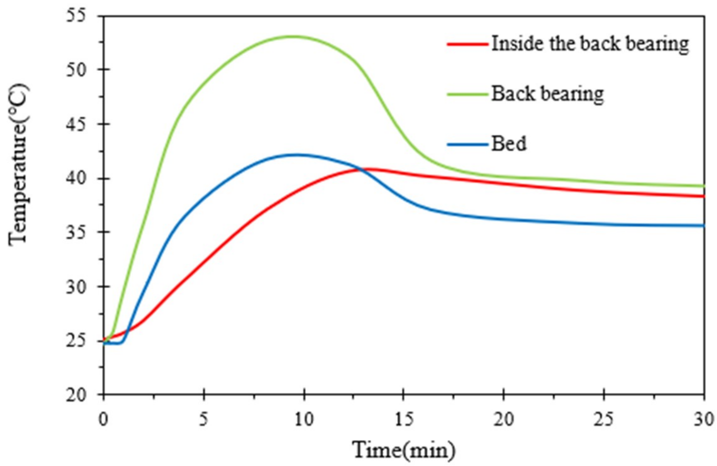

Fig. 8. Three-dimensional model of heating structure

the smallest one (41°C) is inside the bearing. The bearing support for the screw driver is the angular contact ball bearing which can work within temperature range of −40°C to +100°C. Thus, the maximum temperature inside the back bearing is within the allowable temperature range of the bearing.

According to the above analysis, it is demonstrated that the use of PTC plates for rapid heating has no significant influence on working ability and life time of the bearing. Fig. 9 illustrates the actual setup of five PTC plates in the structure. All the heat plates are installed at the fixed end of the screw bearing to control thermal displacement along the screw axis. The generated heat is transferred through the bearing housing and further it heats up the screw until the required displacement is reached.

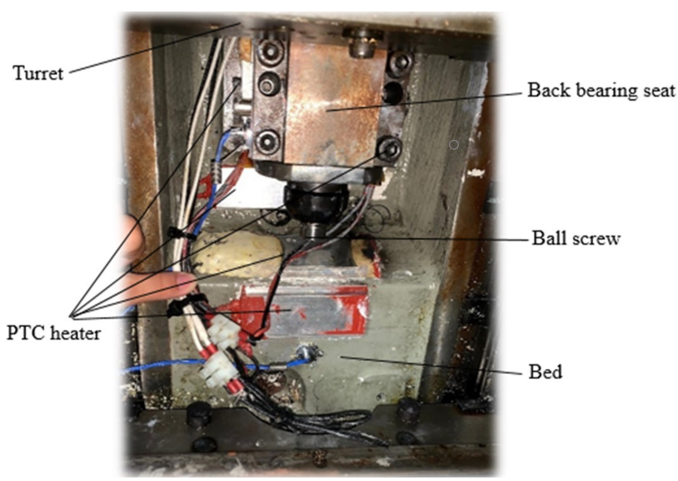

Fig. 9. Predicted temperature distribution on the structure

3. Results and discussions

3.1. Logical control coefficients

As it is known, the X-axis is the main cutting direction of the lathe that has a significant effect on precision of the product diameter. This research aims at using a rapid heating system which causes that thermal displacement along the X-axis achieves stability in a short time. As presented in Section 2.2, the rapid heating is controlled by a logical algorithm, as in Eq. (1), to quickly increase the temperature (and thermal displacement) after the start, and then to maintain the temperature for obtaining the demanded thermal displacement.

To determine the coefficients in Eq. (1), multiple tests for working condition of Case 1 (refer to Table 2) have been performed. According to these tests, the fast-heating time t_{fast}, the temperature increment ΔT and the temperature control coefficient C are 10, 17.5 and 0.04, respectively. Fig. 10 displays experimental results of thermal displacement and temperatures when the machine runs for about 400 minutes with the spindle speed of 1,500 rpm and the feed rate of 6,000 mm/min. The results reveal that thermal displacement in the X-axis decreass in the first 25 minutes; it then tends to increase continuously in the next period of time and cannot reach the steady state (Fig. 10a). The variation range of thermal displacement without rapid heating is about 19.5 µm. Hence, the magnitude of thermal error in the products also changes and is difficult to control or compensate. Fig. 10b shows the thermal displacement and temperatures for the case of using the fast-heating system. It is clear that the thermal displacement quickly reaches the steady state, after only 10 minutes, and then the displacement is maintained and is almost constant. It helps to reduce the time of the warm up process of

Table 2. Experimental conditions of fast heating temperature control

Case	Spindle speed, rpm	Feed rate, mm/min	Ambient temperature, °C	Experiment type
Constant conditions				
1	1500	6000	25.5–29.1	Logic learning
2	1000	3400	23.5–27.7	Low speed, low feed rate
3	1500	3400	24.7–28.9	Medium speed, high feed rate
4	2000	3400	24.6–28.4	High speed, low feed rate
5	1000	8500	25.8–29.3	Low speed, high feed rate
6	1500	8500	26.1–29.2	Medium speed, high feed rate
7	2000	8500	26.3–29.4	High speed, high feed rate
Varying conditions				
8	**1500→500→2000**	**8500**	**28.7–31.8**	**Variable speed**
9	**1500→0→500**	**6000**	**28.7–31.6**	**Lunch break**

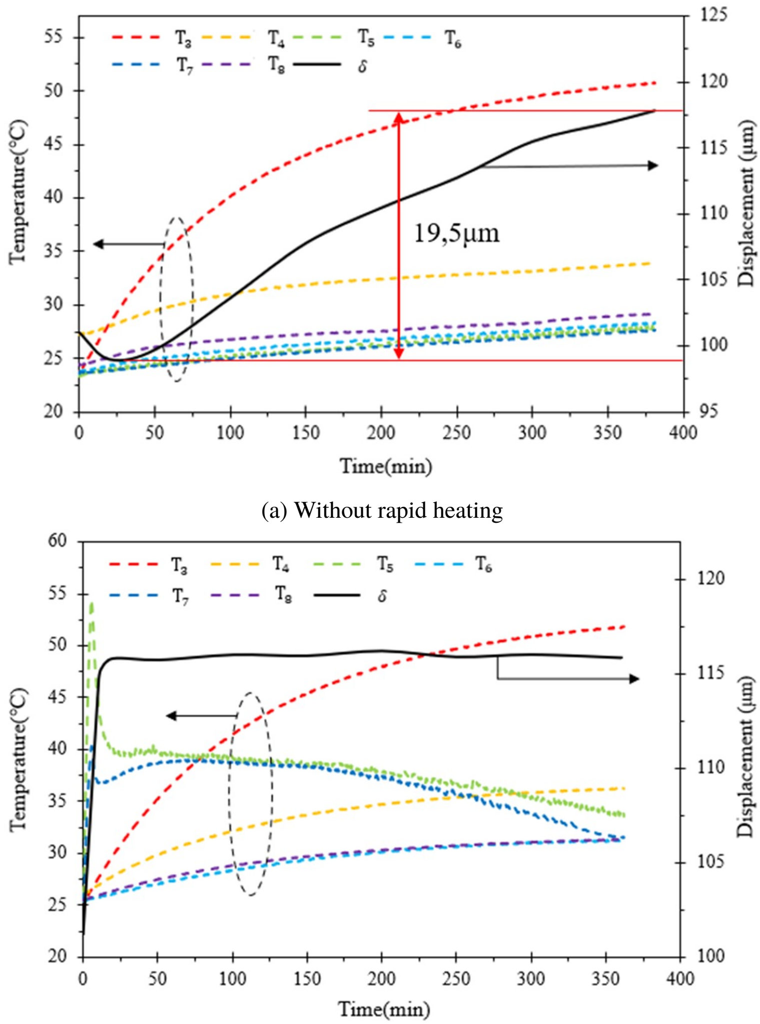

(a) Without rapid heating

(b) With rapid heating

Fig. 10. Time-dependent thermal displacement of X-axis and temperature for the spindle speed of 1,500 rpm and feed rate of 6,000 mm/min

the CNC lathe machine. When the X-axis attains stability, the thermal error is significantly eliminated during checking datum for the machining process, which further improves precision of the machine and accuracy of the products, as well.

3.2. Results for constant working conditions

To consider efficiency of the fast-heating system, other speeds as well as other feed rates, listed in Table 2, have been taken into account by using the determined logical control coefficients. In cases 2 to 7, for each case, the spindle speed and the feed rate are maintained as constant during the testing time (360 minutes). Additionally, since the machine tool doesn't operate in a temperature-controlled room, there could be a random change in ambient temperature. Many researchers [5, 12, 19, 20] have indicated that the ambient temperature has a significant effect on the thermal errors on the machine tools as well as the lathe CNC machine. In the present research, the variable ambient temperature is considered and taken into account in the logical control algorithm. As shown in Table 2, the ambient temperature changed during performing the experiments (23.5°C–31.8°C). For each test, the ambient temperature was also changed when the experiment was implemented. The thermal displacement results obtained for the machine operation with and without the fast-heating system for all working conditions are given in Fig. 11. It can be seen that the thermal displacements mostly decrease during the first 25 minutes and then they continuously increase over the following period of time for the case without the use of the fast-heating system, as shown in Fig. 11a. While, when using the fast-heating system, the thermal displacements become stable only after about 10 minutes, as shown in Fig. 11b.

Normally, the machine tool requires a long time before the machining process for starting and warming up to achieve the steady state. In this study, the rapid heating is introduced to reduce the thermal steady-state time of a machine tool. Therefore, the steady-state time is the first criterion for judging the experimental effect. Secondly, the price of machine tool is determined based on its precision. On the other hand, the displacement after the steady state significantly distributes the machine tool precision; thus it is another criterion. The steady-state time improvement rate r_t and the maximum displacement improvement rate r_δ are defined as follows:

$$r_t = \frac{t_o - t_f}{t_o} 100\%, \tag{8}$$

$$r_\delta = \frac{\Delta\delta_o - \Delta\delta_f}{\Delta\delta_o} 100\%, \tag{9}$$

where t_o and t_f are the original steady-state time and the steady-state time of rapid heating, respectively. The steady-state time refers to the first moment of time when the variation of displacement within one hour is lower than 1 µm; if the displacement does not reach the steady state during the experimental process, then the total time of experiment is assumed as the steady-state time. Similarly, $\Delta\delta_f$ and $\Delta\delta_o$ are, respectively, the maximum displacements for the cases when using and without using the rapid heating; and $\Delta\delta = \delta_{\max} - \delta_{\min}$ represents the difference between maximum displacement $\delta_{\max}$ and minimum displacement $\delta_{\min}$.

Based on the data in Fig. 11, the time improvement and thermal displacement of all operation conditions are computed and listed in Table 3. The results show that the time required for thermal displacement to reach the stable state with the fast-heating system is much smaller than that without the fast-heating system (the original time). The maximum time with the rapid heating is only 20 minutes. For

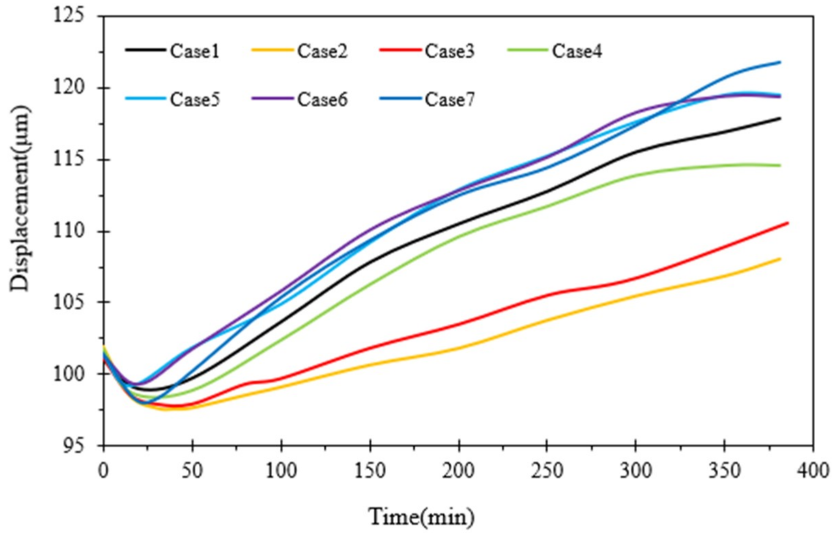

(a) Without the fast-heating system

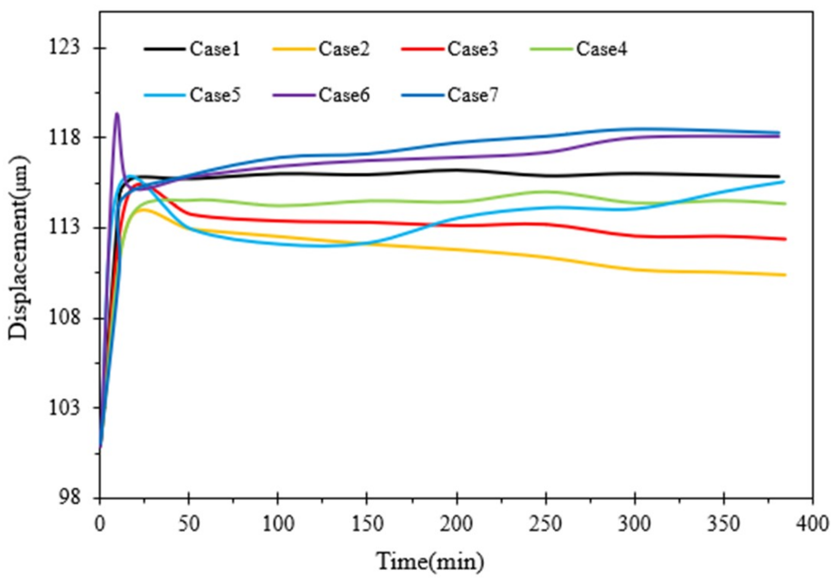

(b) With the fast-heating system

Fig. 11. Experimental thermal displacements

all the cases, the steady-state time is reduced by more than 95% compared to the original time.

In an actual production, the machine tools will be started up in about 10–25 minutes; then the machine will proceed to work. If the machine does not reach a steady state, the thermal error can change and accumulate continuously on the

Table 3. Steady-state time improvement

Case	Time			Thermal displacement		
	t_o (min)	t_f (min)	r_t (%)	$\Delta\delta_o$ (μm)	$\Delta\delta_f$ (μm)	r_δ (%)
1	360	10	97.22	18.84	1.47	92.18
2	360	15	95.83	10.43	2.95	71.71
3	360	17	95.28	12.71	2.47	80.57
4	300	12	96	15.84	1.67	89.43
5	320	20	96.25	20.34	3.45	82.99
6	300	15	96.67	20.24	3.65	81.88
7	360	15	95.83	22.47	3.90	82.62
8	**360**	**12**	**96.67**	9.25	3.5	**62.16**
9	**450**	**15**	**97.33**	10.1	3.4	**66.34**

products. As shown in Table 3, the maximum cumulative error can be up to 18.84 μm for the case without using the rapid heating system. If the fast-heating system is applied, the thermal error is cut down to 1.47 μm which means a reduction by 92.18%. Oscillation amplitude of the thermal error after the rapid heating time in all cases is from 1 μm to 4 μm. Through the experimental results, it is demonstrated that minimum percentage reduction of the thermal errors is 71.71% (in case 2) and in almost all cases thermal errors are diminished by more than 80%.

From the above analysis, it follows that the fast-heating system is highly effective, allowing for achieving the stable thermal error of the X-axis of the CNC lathe in a short time under any combination of constant spindle speed and feed rate.

3.3. Results for varying working conditions

Actually, the machine tools usually work under varying conditions such as the spindle speed, the feed rate, the brake for changing the workpiece or the rest time. Therefore, in this section, some test results for these situations will be presented. To analyze situations similar to the actualones, two working conditions (cases 8 and 9 in Table 2) have been considered.

From Fig. 12a, one can see that the thermal displacement without using the fast-heating system decreases for 50 minutes at the beginning and then it continuously increases until the end of the test. In addition, the spindle speed decreases from 1,000 to 500 rpm in about 120 min. that causes a slow drop in the temperature and in the displacement, as well. On the contrary, after about 240 min, the rotation speed increases to 2,000 rpm which leads to the increase in the temperature and thermal displacement. Thus, without using the fast-heating system, the thermal displacement decreases for the first 50 minutes and then it continuously increases until the end of the test. The total increment of the thermal displacement is about 9.25 μm. However, in the case of using the fast-heating system, the thermal displacement quickly reaches the steady state, after only 10 minutes. Although the temperature control logic cannot completely stabilize the thermal displacement in

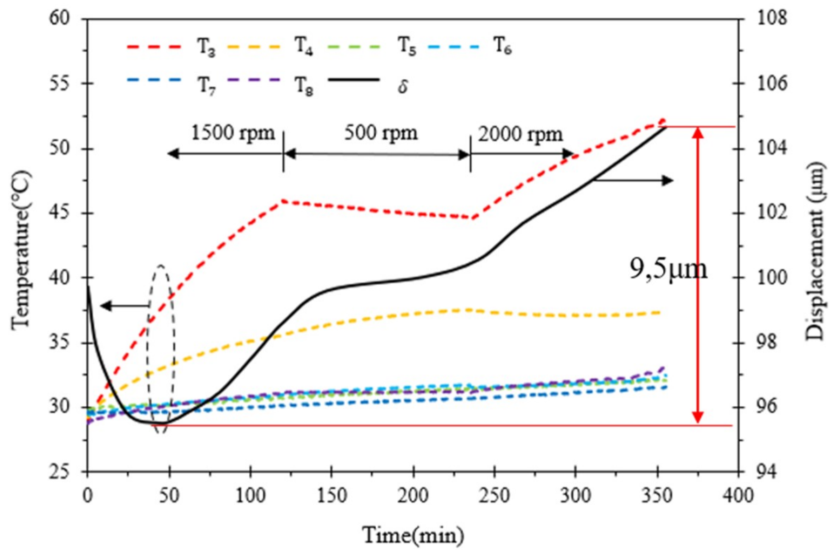

(a) Without rapid heating

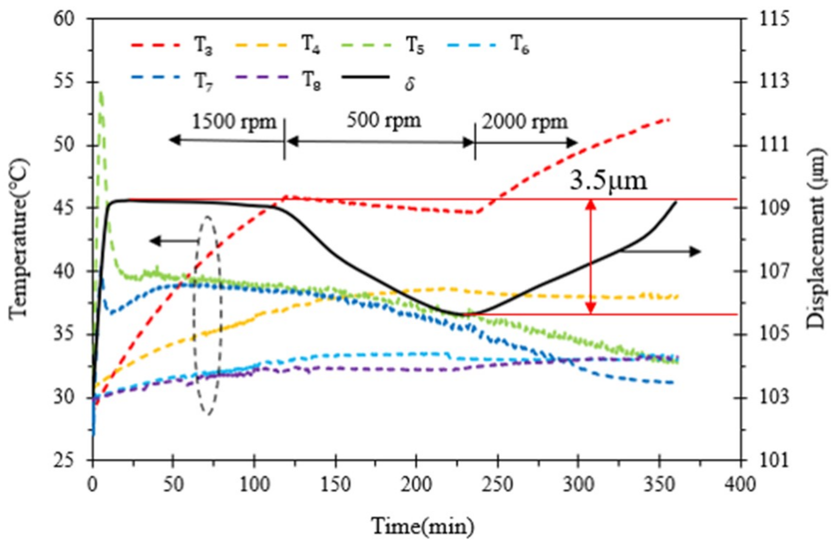

(b) With rapid heating

Fig. 12. Temperature and displacement under varying spindle speeds (Case 8)

the response to a sudden change in the spindle speed, the maximum oscillation amplitude of the thermal displacement is only about 3.5 μm. It means that the thermal displacement is reduced by 62.16% thanks to the use of the fast-heating system (refer to Table 3). Therefore, one can say that the fast-heating system has a good efficiency in controlling the temperature as well as the thermal displacement in the X-axis of the CNC lathe under varying spindle speeds.

Another case is the lunch break time introduced during the working time. This case, with the machine tool working under constant speed and feed rate, is analyzed and depicted in Fig. 13. For 180 minutes of work without the fast-heating system, the results show that the thermal displacement also decreases for the first 25 minutes and then it subsequently grows until the moment of lunch break (for 180 minutes), as displayed in Fig. 13a. During the rest time, the temperatures at different locations have mixed trends; T_3, T_5 to T_8 have downward trends while T_4 has an opposite

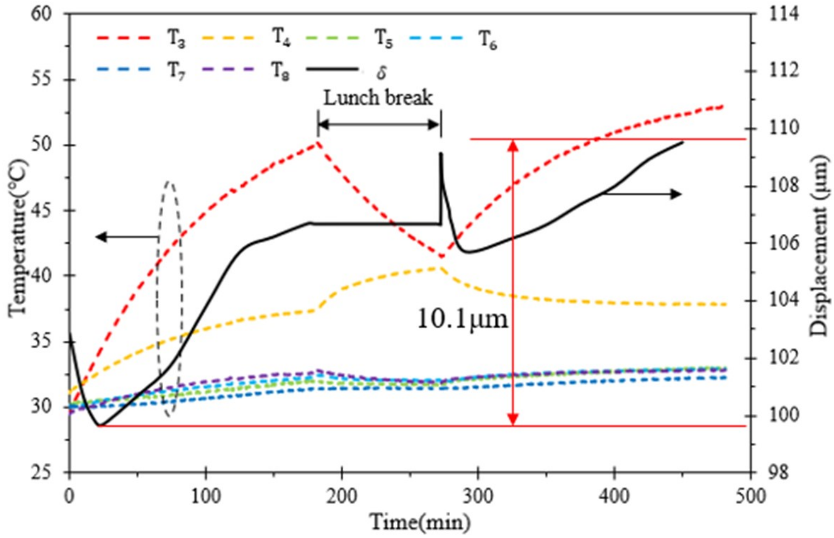

(a) Without rapid heating

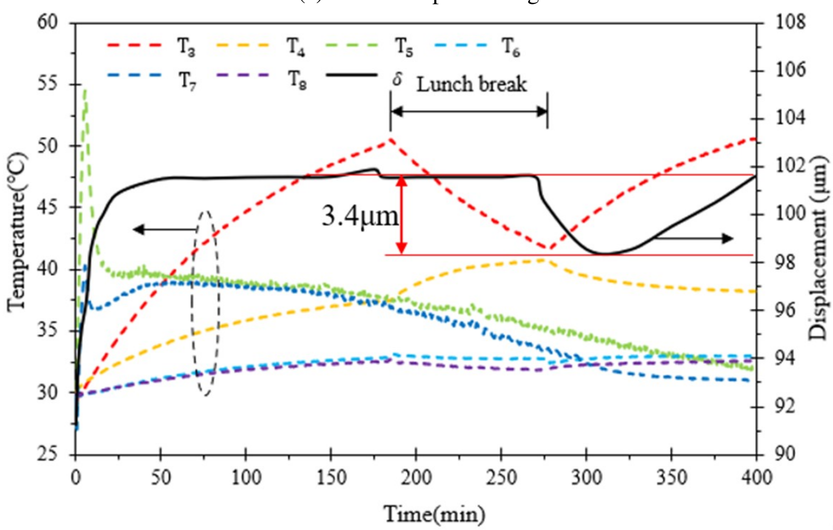

(b) With rapid heating

Fig. 13. Temperature and displacement for the case of included lunch break time (Case 9)

trend. Thus, there is a complex variation of temperature in the machine which leads to a change in thermal displacement, too. The thermal displacement jumps when the machine is back to work after the rest period. This may cause errors in products. Without the temperature control system, the maximum increment of the thermal displacement is 10.1 μm in the total testing time.

With the fast-heating system, the temperatures at T_5, T_6, T_7 and T_8 are controlled to keep the thermal displacement stable. As shown in Fig. 13b, the thermal displacement quickly reaches the steady state and then remains almost unchanged. After the lunch break time, the recorded thermal error is decreasing. However, until the thermal displacement achieves the steady state, its maximum variation range is 3.4 μm. It demonstrates the that rapid heating system still has a good effectiveness in controlling the thermal displacement in the X-axis, reducing it by about 66.34%.

Based on the analysis of the thermal error in the X-axis for the variable working conditions, one can state that the efficiency of control is lower than that for constant operation parameters. However, this efficiency is still satisfactory, and the applied equipment is a simpler solution than the intervention into the numerical control system in the CNC lathe machine for compensation of thermal errors.

4. Conclusions

In this study, a heating system to control the temperature which results on thermal displacement of the X-axis in the CNC lathe machine is successfully constructed. A rapid heating module including a Microprocessor Control Unit, a hardware, thermocouples, etc. is developed and implemented based on a logical algorithm. The operation of the rapid heating system is performed in two stages: quickly increasing the temperature in order to make the thermal displacement achieving the steady sate in short time, and keeping stability of the thermal error. To avoid an excessive grows of temperature, which may cause diminishing of the bearing fatigue life, a numerical temperature distribution analysis has been done in the entire structure for the conditions of maximum power supply. The results indicate that maximum temperature inside a bearing is about 41°C, which is in normal range for the bearing. Both constant and variable operating conditions are tested. Comparing the operation without and with the heating control system, it demonstrated that the warm up time and the thermal displacement are reduced by more than 95% and 80%, respectively, under constant working conditions; and also above 95% and 60%, respectively, for varying working conditions. Moreover, it is clear that the rapid heating model is effective in both cases, even in different ambient temperatures and varying ambient temperature. So, it is not necessary to build a sophisticated thermal compensation model connected to the controller of the machine tool. Hence, the fast-heating system can be applied in the CNC lathe to reduce the thermal error, which will help to improve the machine's precision.

Acknowledgements

This study was financially supported by the Outlay MOST 109-2221-E-035-006-MY2 given by Ministry of Science and Technology, Taiwan, R.O.C.

References

[1] J. Bryan. International status of thermal error research. *CIRP Annals*, 39(2):645–656, 1990. doi: 10.1016/S0007-8506(07)63001-7.

[2] J. Mayr, J. Jedrzejewski, E. Uhlmann, M. Alkan Donmez, W. Knapp, F. Härtig, et al. Thermal issues in machine tools. *CIRP Annals*, 61(2):771–791, 2012. doi: 10.1016/j.cirp.2012.05.008.

[3] H. Wang, F. Li, Y. Cai, Y. Liu, and Y. Yang. Experimental and theoretical analysis of ball screw under thermal effect. *Tribology International*, 152:106503, 2020. doi: 10.1016/j.triboint.2020.106503.

[4] C. Jin, B. Wu, and Y. Hu. Heat generation modeling of ball bearing based on internal load distribution. *Tribology International*, 45(1):8–15, 2012. doi: 10.1016/j.triboint.2011.08.019.

[5] J. Liu, C. Ma, S. Wang, S. Wang, B. Yang, and H. Shi. Thermal boundary condition optimization of ball screw feed drive system based on response surface analysis. *Mechanical Systems and Signal Processing*, 121:471–495, 2019. doi: 10.1016/j.ymssp.2018.11.042.

[6] C.-H. Wu and Y.-T. Kung. Thermal analysis for the feed drive system of a CNC machine center. *International Journal of Machine Tools and Manufacture*, 43(15):1521–1528, 2003. doi: 10.1016/j.ijmachtools.2003.08.008.

[7] H. Shi, C. Ma, J. Yang, L. Zhao, X. Mei, and G. Gong. Investigation into effect of thermal expansion on thermally induced error of ball screw feed drive system of precision machine tools. *International Journal of Machine Tools and Manufacture*, 97:60–71, 2015. doi: 10.1016/j.ijmachtools.2015.07.003.

[8] W.S. Yun, S.K. Kim, and D.W. Cho. Thermal error analysis for a CNC lathe feed drive system. *International Journal of Machine Tools and Manufacture*, 39:1087–1101, 1999. doi: 10.1016/S0890-6955(98)00073-X.

[9] H. Shi, B. He, Y. Yue, C. Min, and X. Mei. Cooling effect and temperature regulation of oil cooling system for ball screw feed drive system of precision machine tool. *Applied Thermal Engineering*, 161:114150, 2019. doi: 10.1016/j.applthermaleng.2019.114150.

[10] Z.Z. Xu, X.J. Liu, H.K. Kim, J.H. Shin, and S.K. Lyu. Thermal error forecast and performance evaluation for an air-cooling ball screw system. *International Journal of Machine Tools and Manufacture*, 51(7-8):605–611, 2011. doi: 10.1016/j.ijmachtools.2011.04.001.

[11] S.-C. Huang. Analysis of a model to forecast thermal deformation of ball screw feed drive systems. *International Journal of Machine Tools and Manufacture*, 35,(8):1099–1104, 1995. doi: 10.1016/0890-6955(95)90404-A.

[12] T.-J. Li, J.-H. Yuan, Y.-M. Zhang, and C.-Y. Zhao. Time-varying reliability prediction modeling of positioning accuracy influenced by frictional heat of ball-screw systems for CNC machine tools. *Precision Engineering*, 64:147–156, 2020. doi: 10.1016/j.precisioneng.2020.04.002.

[13] C. Ma, J. Liu, and S. Wang. Thermal error compensation of linear axis with fixed-fixed installation. *International Journal of Mechanical Sciences*, 175:105531, 2020. doi: 10.1016/j.ijmecsci.2020.105531.

[14] J. Zapłata and M. Pajor. Piecewise compensation of thermal errors of a ball screw driven CNC axis. *Precision Engineering*, 60:160–166, 2019. doi: 10.1016/j.precisioneng.2019.07.011.

[15] W. Feng, Z. Li, Q. Gu, and J. Yang. Thermally induced positioning error modelling and compensation based on thermal characteristic analysis. *International Journal of Machine Tools and Manufacture*, 93:26–36, 2015. doi: 10.1016/j.ijmachtools.2015.03.006.

[16] H. Zhou, P. Hu, H. Tan, J. Chen, and G. Liu. Modelling and compensation of thermal deformation for machine tool based on the real-time data of the CNC system. *Procedia Manufacturing*, 26:1137–1146, 2018. doi: 10.1016/j.promfg.2018.07.150.
[17] A.A. Kendoush. An approximate solution of the convective heat transfer from an isothermal rotating cylinder. *International Journal of Heat and Fluid Flow*, 17(4):439–441, 1996. doi: 10.1016/0142-727X(95)00002-8.
[18] T.L. Bergman, F.P. Incropera, D.P. DeWitt, and A.S. Lavine. *Fundamentals of Heat and Mass Transfer*. 7th edition, John Wiley & Sons, 2011.
[19] Z. Li, K. Fan, J. Yang, and Y. Zhang. Time-varying positioning error modeling and compensation for ball screw systems based on simulation and experimental analysis. *The International Journal of Advanced Manufacturing Technology*, 73:773–782, 2014. doi: 10.1007/s00170-014-5865-9.
[20] J.G. Yang, Y.Q. Ren, and Z.C. Du. An application of real-time error compensation on an NC twin-spindle lathe. *Journal of Materials Processing Technology*, 129(1-3):474–479, 2002. doi: 10.1016/S0924-0136(02)00618-0.